



## The use of aptamers and molecularly imprinted polymers in biosensors for environmental monitoring: A tale of two receptors

Naseri, Maryam; Mohammadniaei, Mohsen; Sun, Yi; Ashley, Jon

*Published in:*  
Chemosensors

*Link to article, DOI:*  
[10.3390/CHEMOSENSORS8020032](https://doi.org/10.3390/CHEMOSENSORS8020032)

*Publication date:*  
2020

*Document Version*  
Publisher's PDF, also known as Version of record

[Link back to DTU Orbit](#)

### *Citation (APA):*

Naseri, M., Mohammadniaei, M., Sun, Y., & Ashley, J. (2020). The use of aptamers and molecularly imprinted polymers in biosensors for environmental monitoring: A tale of two receptors. *Chemosensors*, 8(2), Article 32. <https://doi.org/10.3390/CHEMOSENSORS8020032>

---

### General rights

Copyright and moral rights for the publications made accessible in the public portal are retained by the authors and/or other copyright owners and it is a condition of accessing publications that users recognise and abide by the legal requirements associated with these rights.

- Users may download and print one copy of any publication from the public portal for the purpose of private study or research.
- You may not further distribute the material or use it for any profit-making activity or commercial gain
- You may freely distribute the URL identifying the publication in the public portal

If you believe that this document breaches copyright please contact us providing details, and we will remove access to the work immediately and investigate your claim.

Review

# The Use of Aptamers and Molecularly Imprinted Polymers in Biosensors for Environmental Monitoring: A Tale of Two Receptors

Maryam Naseri, Mohsen Mohammadniaei , Yi Sun \* and Jon Ashley \* 

Department of Healthcare Technology, Denmark Technical University, 2800 Kgs. Lyngby, Denmark; maryn@dtu.dk (M.N.); mohmo@dtu.dk (M.M.)

\* Correspondence: suyi@dtu.dk (Y.S.); jash@dtu.dk (J.A.)

Received: 29 March 2020; Accepted: 1 May 2020; Published: 6 May 2020



**Abstract:** Effective molecular recognition remains a major challenge in the development of robust receptors for biosensing applications. Over the last three decades, aptamers and molecularly imprinted polymers (MIPs) have emerged as the receptors of choice for use in biosensors as viable alternatives to natural antibodies, due to their superior stability, comparable binding performance, and lower costs. Although both of these technologies have been developed in parallel, they both suffer from their own unique problems. In this review, we will compare and contrast both types of receptor, with a focus on the area of environmental monitoring. Firstly, we will discuss the strategies and challenges involved in their development. We will also discuss the challenges that are involved in interfacing them with the biosensors. We will then compare and contrast their performance with a focus on their use in the detection of environmental contaminants, namely, antibiotics, pesticides, heavy metals, and pathogens detection. Finally, we will discuss the future direction of these two technologies.

**Keywords:** aptamer; molecularly imprinted polymers; environmental contaminants; heavy metal; pathogens; antibiotics

## 1. Introduction

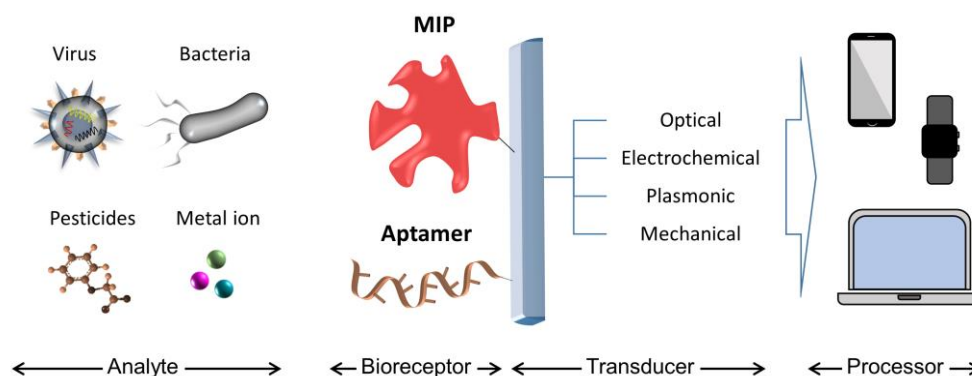
Biomimetic binders have come to the forefront of biotechnology as a potential replacement of animal derived antibodies and they have seen widespread use in a large number of different applications, including as transduction elements in biosensing devices (Scheme 1) [1]. The two main classes of biomimetic receptors, namely aptamers and molecularly imprinted polymers (MIPs) have garnered the most interest by researchers over the last two decades. In particular, researchers have applied both of these technologies in the detection of environmental contaminants to address the current gap for reliable ligands that are capable of binding small molecule contaminants. Aptamers are ssDNA or RNA recombinant oligonucleotides that form distinct conformational shapes, which are complementary to the target molecule. MIPs are synthetic polymers, which contain complimentary cavities (recognition sites), which can rebind to the template molecule. When comparing antibodies to both aptamers and molecularly imprinted polymers, the latter two technologies have shown distinct advantages (Table 1). MIPs and aptamers are both, in general, more stable when compared to natural antibodies, demonstrating extended shelf lives. Both technologies show comparable binding performance to natural antibodies or even outperform them in some instances. Aptamers can be modified in several different ways to improve functionalities, such as replacing the phosphate backbone to improve their bioavailability, resist nuclease enzyme degradation, or increase the non-natural interactions of DNA/RNA with the analyte molecule [2,3]. For example, we can introduce hydrophobic interactions by adding a hydrophobic moiety to the aptamers either through post SELEX modification or during

selection, which can enhance the specific binding performance [4]. This is critical, as DNA/RNA is mostly hydrophilic in nature and, as such, the contribution of hydrophobic interactions in unmodified aptamers is minimal. Additional functionality can be introduced to aptamers through the tagging at the 5' or 3' ends with functional molecules, such as fluorophores or biotin [5]. The ability to modify aptamers is especially important when applying aptamers in *in vivo* applications, such as drug therapeutics and drug delivery, where unmodified aptamers are particularly susceptible to enzyme degradation. It could also be crucial to modify aptamers for use in environmental monitoring of environmental samples, where DNA/RNA is susceptible to degradation, due to a number of environmental parameters [6].

In the case of MIPs, different functionalities can be introduced via the inclusion of functional monomers into the pre-polymerisation mixtures or performing additional polymerisation steps [7]. Unlike antibodies, both aptamers and MIPs show good stability and extended shelf lives. MIPs can also be synthesized as a bulk material, nanocomposite, thin film, or act as nanomaterials in their own right (nanoMIPs) [8–10].

This tailorability of both MIPs and aptamers makes them particularly useful and versatile as biomimetic binders in biosensors and as capture agents for sample pre-treatment applications, including food monitoring and environmental monitoring.

In this review, we aim to compare and contrast the various key performance criteria of MIPs and aptamers, as receptors for sensors in the environmental monitoring of pollutants with a focus on antibiotic residues, heavy metals, and pathogens as a representative cross section of targets for both technologies. We will also discuss the future directions of both these technologies. The review covers the developments of the last 5–10 years of aptamer and MIP development with selected examples of environmental contaminants, where MIPs and aptamers have both been utilized in biosensors.



**Scheme 1.** Aptamer and molecularly imprinted polymer (MIP) for environmental pollutant detection.

### 1.1. The Development of Aptamers and MIPs

The methods used to synthesize MIPs and aptamers are completely different in terms of the considerations used for their development. Aptamers are selected from a random library of oligonucleotides containing a random region of 20–60 nucleotides with a constant region that is located on both sides in a combinatorial approach known as Systematic Evolution of Ligands by Exponential enrichment (SELEX) or *in vitro* selection. This method involves repeated rounds of partitioning, amplification, and regeneration of target bound ssDNA or RNA [11]. After a certain number of rounds (8–20 rounds), an enriched library containing about  $10^3$  unique sequences is achieved and sequenced to identify binding nucleic acid candidates.

MIPs are synthesized via molecular imprinting, whereby the target is incubated with functional monomers to form non-covalent interactions in the pre-polymerisation mixture. Upon subsequent cross-linking, a cavity is formed and the removal of the template leaves a recognition site for the target molecule to rebind. More classical methods involved the so called covalent imprinting, where the template is attached to a monomer via a reversible covalent bond. Upon imprinting, the template is

removed [12]. This technique is no longer commonly used, with researchers opting for the non-covalent imprinting strategies. MIPs can be synthesized into a number of different morphologies, including bulk materials, nanomaterials, nanocomposites, or thin films [13–15]. Traditionally, MIPs were formed using bulk polymerization as a sorbent for solid-phase extraction via the formation of large size MIP monoliths. These monoliths were then ground up into smaller particles and packed into the column. Subsequent methods for imprinting MIP based nanoparticles and nanomaterials have gained prominence and allowed for small nano-sized MIPs with good yields and controllable sizes, such as solid-phase synthesis, emulsion, and precipitation polymerization [16–18]. For larger targets, epitope imprinting has shown promise as a viable way to imprint larger templates [19]. When compared to aptamers, MIPs can be rationally designed in a bottom-up manner using a number of techniques, including computational modelling and experimental methods [20,21].

**Table 1.** Antibodies vs. MIPs vs. Aptamers.

Antibodies	MIPs	Aptamers
<b>Methods for Development</b>		
<b>Immune response in animal host:</b>	<b>Molecular imprinting:</b>	<b>SELEX:</b>
<ul style="list-style-type: none"> <li>• Several Months</li> <li>• Expensive</li> <li>• High immunological response needed</li> <li>• Any target (in vivo)</li> <li>• Animals needed</li> </ul>	<ul style="list-style-type: none"> <li>• Several weeks</li> <li>• Cheap</li> <li>• Trial and error or rational design</li> <li>• Small molecule template (organic solvents), protein and cells (aqueous solution)</li> </ul>	<ul style="list-style-type: none"> <li>• Several weeks</li> <li>• Expensive</li> <li>• Combinatorial Screening with Post SELEX modification</li> <li>• Any target (aqueous solution)</li> </ul>
<b>Production</b>		
<b>Immune Response in Animals:</b>	<b>Molecular Imprinting:</b>	<b>Solid-phase synthesis:</b>
<ul style="list-style-type: none"> <li>• High batch-to-batch variation</li> <li>• Amino acid interactions</li> <li>• Limited functionality</li> <li>• End labelling possible</li> <li>• Low yields</li> <li>• Antigen required every time</li> </ul>	<ul style="list-style-type: none"> <li>• Moderate batch-to-batch variation</li> <li>• A large number of Functional monomers and interactions available</li> <li>• High functionality and tailorability</li> <li>• Non-specific labelling</li> <li>• Template dependent yield and cost</li> <li>• Template removal required</li> </ul>	<ul style="list-style-type: none"> <li>• Low batch-to-batch variation.</li> <li>• Hydrogen bonding, electrostatic and G-Quadruplex structures</li> <li>• Functionality through chemical modification of structural DNA/RNA</li> <li>• End labelling possible</li> <li>• High Yields</li> <li>• Cheap to synthesize</li> <li>• Template free synthesis</li> <li>• Cheap to synthesize</li> </ul>
<b>Properties</b>		
<b>Binding Affinity:</b>	<b>Binding Affinity:</b>	<b>Binding Affinity:</b>
<ul style="list-style-type: none"> <li>• Small molecule targets (Low)</li> <li>• Protein and Cell targets (High)</li> </ul>	<ul style="list-style-type: none"> <li>• Small molecule targets (high)</li> <li>• Protein and Cell targets (High)</li> </ul>	<ul style="list-style-type: none"> <li>• Small molecule targets (Moderate)</li> <li>• Protein and Cell targets (High)</li> </ul>
<b>Specificity:</b>	<b>Specificity:</b>	<b>Specificity:</b>
<ul style="list-style-type: none"> <li>• Small molecule targets (low)</li> <li>• Protein and Cell targets (High)</li> </ul>	<ul style="list-style-type: none"> <li>• Small molecule targets (High)</li> <li>• Protein and Cell targets (Low)</li> </ul>	<ul style="list-style-type: none"> <li>• Small molecule targets (High)</li> <li>• Protein and Cell targets (High)</li> </ul>
<b>Stability:</b>	<b>Stability:</b>	<b>Stability:</b>
<ul style="list-style-type: none"> <li>• Low (Months)</li> </ul>	<ul style="list-style-type: none"> <li>• High (Years)</li> </ul>	<ul style="list-style-type: none"> <li>• High (Years)</li> </ul>
<b>Size:</b>	<b>Size:</b>	<b>Size:</b>
<ul style="list-style-type: none"> <li>• &lt;12–15 nm</li> </ul>	<ul style="list-style-type: none"> <li>• 3–5 nm</li> </ul>	<ul style="list-style-type: none"> <li>• 50 nm to 100 <math>\mu</math>m</li> </ul>

Aptamers, on the other hand, can only undergo rational design after their selection (post-selection modification) [22].

Both technologies have shown limitations in the methods used for their development, which has hindered their commercial development. However, a number of companies have started selling both of these technologies. In terms of the commercialization of aptamers, several companies are offering aptamer selection services and aptamer based immunoassays [23]. In addition, aptamers have been successfully developed as therapeutics in their own right [24]. In terms of MIPs, a number of companies have been established, such as PolyIntell, Biotage, Supelco to sell MIPs for solid phase extraction, and MIP Diagnostics in the UK, offering custom MIP based receptors development services. Furthermore,

Wheatley SPI, LLC recently developed a MIP based commercial test device, called SAFE-T<sup>®</sup>, for the detection of explosives [25].

A scan of the literature for both MIPs and aptamers for different types of target suggest that they show contrasting binding performance [26]. For instance, the development of MIPs targeting small molecules is now considered routine, while the selection of aptamers for small molecules is more of a challenge due to the difficulty in separating small molecule-aptamer binding complexes from the DNA library. This is due to the lack of mass-transfer (lack of size difference between bound and unbound DNA) upon binding of the small molecule. Although it is worth noting that structure switching protocols (Reverse SELEX) have overcome this problem through the docking of the DNA library onto a solid phase [27]. Upon binding of the small molecule target, to any sequences within a library, the aptamer undergoes a change in conformation and elutes off the solid phase. It is also worth noting that the binding affinities displayed by aptamers against small molecules can vary between targets but have demonstrated high specificity [28]. The development of chemically modified aptamers for small molecules is further complicated by their poor PCR efficiency, with only a handful of chemically modified aptamers being developed for small molecules to date [29]. In addition, the PCR bias effect can also reduce the chances of screening high affinity binders [30]. This occurs because, during repeated rounds of selection, certain sequences become over represented in the final sequence data due to certain sequences being easier to amplify. A number of non-SELEX based methods have been developed that can overcome this issue [31].

MIPs, on the other hand, can suffer from high non-specific binding in the sample matrix as well as template leakage, which means that some of the template is not removed after synthesis, leading to false positive results [32,33]. However, the use of dummy templates has helped to prevent template leakage [34]. It is worth noting that the methods used to measure the binding properties and binding models used for both aptamers and MIPs are completely different [35–37]. A reverse in binding performance is seen as we increase the size of the target molecule, whereby the binding affinities for aptamers generally increase while MIPs start to suffer from performance issues in terms of specificity, due to the lack of compatible monomers and increased chances of non-specific binding [38,39]. This non-specific binding is due to the large surface area available around the MIP material, which can act as sites for non-specific interactions with the sample matrix and structurally related analytes and the lack of accessibility on the MIP surface for larger templates, such as cells and proteins. It is also worth noting that aptamers selected against whole cell or virus targets using either the whole cell-SELEX or SELEX against the target membrane antigens can suffer from significant non-specific binding, due to the large number of possible membrane protein antigen binding sites available on a pathogen that may be common across several species [40]. As aptamers fold into three-dimensional (3D) conformations, which can be dependent on a number of parameters, such as temperature, and salt concentration, their performance can vary if the buffer conditions used deviate from the original buffer conditions used during the selection. The same can be said for MIPs, where the choice of organic solvent (porogen) can drastically affect the final MIP performance and structural properties of the MIP molecules [41].

Comparing the methods used to develop both MIPs and aptamers, the SELEX methodology appears to be more convoluted, time consuming, and costly when compared to the synthesis of MIPs, which just requires a synthesis step, template removal step, and binding validation. Their development is often achieved through a trial and error approach to find the optimal monomer to template to cross linker ratios, although the use of rational design in MIP development is becoming increasingly important [42]. On the other hand, once aptamers have been successfully selected and the sequences elucidated, the cost of their production rapidly decreases due to relatively cheap costs of DNA synthesis. This is in comparison to MIPs, which always require an equimolar amount of template to form the molecular recognition sites on the MIPs.

Interestingly, researchers have looked at combining the properties of MIPs and aptamers to improve upon their binding properties to overcome some of the issues that are associated with them [43,44].

### 1.2. Interfacing Aptamers and MIPs to the Sensor Surface

One of the most important considerations for the development of a biosensor is how to attach the recognition element to the sensor surface. The ability to attach different tags to aptamers at the 5' or 3' end, including biotin, thiol groups etc., has made their bio-conjugation to the sensor surface relatively straight forward via coupling reactions annealing to a DNA probe or adsorption [45]. On the other hand, the conjugation of MIPs is more challenging. MIPs can either be formed on the surface of the sensor as a film or mixed with a nanocomposite material in the case for electrochemical based methods, which use electro polymerization methods [8,46]. In some cases, additional polymerisation to attach functional groups to the outside of the MIP can be performed, as is the case for solid-phase synthesis prior to conjugation [47,48]. However, there is little control over where these functional groups are on the MIP.

## 2. Aptamers and MIPs in the Detection of Small Molecule Contaminants

### 2.1. Antibiotics

The accumulation of antibiotic residues in the environment has become an increasing concern, due to the increasing likelihood that microbials develop antibiotic resistance to our frontline drugs and can accumulate in wildlife. Aptamers and MIPs have both been utilised as receptors in biosensors, which target antibiotics in environmental samples. Out of all the biosensors, developed for antibiotic detection, tetracycline based antibiotic analytes have been the focus of the majority of MIP and aptamer based biosensors. Recently, Dong et al. demonstrated the use of a photoelectrochemical aptasensor for the detection of tetracycline in environmental samples [49]. Aptamers were immobilized onto Au/BiOI composites via a sulphur gold bond and transduction was achieved through the generation of photoelectrons. The sensor demonstrated a detection limit of  $0.2 \text{ ng L}^{-1}$  (450 fM). In comparison, Clarindo et al. synthesized MIPs for tetracycline, which was ground up and mixed with graphite-polyurethane composite electrode. The subsequent developed sensor demonstrated in the detection of tetracycline in different samples achieved a detection limit of  $0.555 \text{ }\mu\text{M}$  [50]. MIPs and aptamers have both also been demonstrated in fluorescence based optical sensors for the detection of tetracycline based antibiotics. In 2016, researchers developed a hybrid MIP/quantum dot/mesoporous silica based nanocomposite for the detection of tetracycline through fluorescence quenching, which demonstrated a detection limit of  $15.0 \text{ ng mL}^{-1}$  ( $0.0337 \text{ }\mu\text{M}$ ) [51]. In contrast, fluorescence based aptasensors are often simpler in design, due to the ability to tag the fluorophore directly onto the aptamer or the reliance on the displacement of DNA as a basis for the signal transduction. For example, in 2015, researchers demonstrated the detection of tetracycline while using a simple triple helix molecular switch for the detection of tetracycline in tap water, achieving a detection limit of  $2.09 \text{ nM}$  [52]. In addition to tetracycline based antibiotics, aptamers and MIP based sensors have both been developed for other types of antibiotics, such as amoxicillin [53,54]. In the case of kanamycin, Geng et al. even demonstrated the synergistic combination of MIPs and aptamers for the detection of kanamycin while using fluorescence quenching [55]. Overall, there has been a lot of interest in the development of both MIPs and aptamers in the detection of antibiotic residues and both technologies seem to show comparable performance in terms of sensitivity and selectivity.

### 2.2. Pesticides

The overuse of pesticides has become a major source of environmental contamination in water sources [56]. As such, the number of aptamer and MIP based biosensors for the detection of pesticides reported in the literature has grown in recent years [57,58]. However, the availability of

aptamers targeting pesticides is limited to date, due to the challenges that are associated with selecting small molecules.

A higher number of biosensors utilizing MIP based receptors have been reported for the detection of pesticides, partly due to the convenience of synthesizing MIPs. Recently, Weerathunge et al. demonstrated the use of a nanozyme based sensor and aptamer for the detection of chlorpyrifos down to 11.3 ppm (32  $\mu\text{M}$ ) [59]. The nanozyme, based on Ag nanoparticles were found to catalyze the 3,30,5,50-tetramethylbenzidine (TMB) substrate, leading to a colour change. Upon adsorption of the aptamer, the catalysis of the reaction switches off. This catalytic function of the nanozyme can be switched on through the presence of chlorpyrifos, which causes the aptamer to elute off the nanozyme. In comparison, a recent report demonstrated the use of a MIP based electrochemical sensor for the detection of chlorpyrifos [60]. Multi-walled carbon nanotube doped molecularly imprinted silica nanospheres were synthesized and applied onto a glassy carbon electrode and achieved a detection limit of 100 fM. In the case of pesticides, MIPs have clearly shown better performance when compared to aptamers, although this difference might be due to differences in the performance of different biosensor platforms. It is also worth noting that there is a lack of aptamers available for pesticides meaning that the majority of examples of biosensors for pesticide detection has focused on the utilization of MIP based receptors rather than aptamers.

### 2.3. Heavy Metals

Heavy metal contamination has been a global environmental issue because of its toxicity and widespread uses. Because heavy metals are not biodegradable, they can bioaccumulate into organisms and humans under the biological amplification of the food chain. The permitted limit of heavy metals in water sources is typically in the low ng/L concentration range, so that the monitoring of these pollutants in the water environment remains an on-going challenge for environmental chemistry. Both aptamers and ion-imprinted polymers (IIPs), as highly selective receptors, would be good candidates for the detection of trace amounts of heavy metals. In this part, we review recent developments in aptasensors and IIP-based sensors used for the detection of heavy metals (Tables 2 and 3).

#### 2.3.1. Cadmium Sensing

Cadmium contamination in drinking water is mainly caused by cadmium released from the steel and battery industry to the environment via wastewater. The kidney is the main target organ that is affected by cadmium toxicity. The maximum contaminant levels of cadmium in drinking water was defined as 3  $\mu\text{gL}^{-1}$  and 5  $\mu\text{gL}^{-1}$  by the World Health Organization (WHO) and United States Environment Protection Agency (EPA), respectively [61,62]. Colorimetric methods are attractive analysis approaches for  $\text{Cd}^{2+}$  detection, because of their simplicity, short detection times, and low cost. In this regard, Huang et al. introduced a IIP-paper platform as a detection element for colorimetric detection of  $\text{Cd}^{2+}$  ions [63] without complex sample pretreatment and expensive instrumentation. Firstly, thin print paper was oxidized by hydrogen peroxide to introduce enough hydroxyl groups and is then grafted with a reversible addition-fragmentation chain transfer (RAFT) agent. Finally, polymerization took place on the surface of the print paper by the RAFT strategy while using cadmium ions as the template, methylacrylic acid and polyethyleneimine as the monomers. Recently, a colorimetric method based on aptamer-functionalized gold nanoparticles for specific recognition of  $\text{Cd}^{2+}$  was developed [64]. By introducing  $\text{Cd}^{2+}$  ions, the amount of free aptamer decreased because of specific interaction between aptamers and  $\text{Cd}^{2+}$  ions, which led to the lower stability of the AuNPs and resulted in the color change in the solution. A self-developed smartphone-based colorimetric system was employed to capture the colorimetric image of AuNPs solutions before and after adding  $\text{Cd}^{2+}$  and to analyze colorimetric change, which fulfils the quantitative detection of  $\text{Cd}^{2+}$ .

Table 2. Detection of heavy metals using aptasensors.

Aptasensor	Analyte	Detection Method	Linear Range $\mu\text{g L}^{-1}$	LOD $\mu\text{g L}^{-1}$	Ref.
5'-GGGAGGGAAGTGTGTTGGTATTATTTTTGGTTGTGCAGTAGGGCGGG-3'	Cd <sup>2+</sup>	Fluorescence	$0.112 \times 10^1 - 0.224 \times 10^3$	0.34	[65]
5'-HS-(CH <sub>2</sub> ) <sub>6</sub> -TTTCTTCTTTCTTCCCCCTTGTGTTT-Methylene Blue-3'	Hg <sup>2+</sup>	ATR-SEIRAS	$0.1 \times 10^2 - 0.5 \times 10^5$ *	$0.1 \times 10^2$ *	[66]
5'-FAM-GGGTGGGTGGGTGGGT-3'	Pb <sup>2+</sup>	FRET	$0.5 \times 10^{-2} - 0.2 \times 10^2$ *	$0.5 \times 10^{-3}$ *	[67]
5'-GGGTGGGTGGGTGGGT-(CH <sub>2</sub> ) <sub>6</sub> -NH <sub>2</sub> -3'	Pb <sup>2+</sup>	DPV	$0.1 \times 10^{-3} - 0.1 \times 10^3$ *	$0.32 \times 10^{-4}$ *	[68]
[5' ThioMC6-D/TT TCT TCT TTC TTC CCC CCT TGT TTG TTT 3']	Hg <sup>2+</sup>	PEIS	$0.5 \times 10^1 - 0.1 \times 10^6$ (water) $0.5 \times 10^1 - 0.1 \times 10^3$ (DMSO)	$0.1 \times 10^2$ (water) $0.5 \times 10^1$ (DMSO)	[69]
2is5'-FAM-CTCAGGACGACGGGTTCA-CAGTCCGTTGTC-3'	Cd <sup>2+</sup>	Fluorescence	-	$0.4 \times 10^2$ *	[70]
C-PS2.M: CCCTTAATCCCCTTTGTGGGTAGGGCGGGTTGGAAACCTTAATCCCC	Cd <sup>2+</sup>	Fluorescence	$0.5 \times 10^1 - 0.5 \times 10^2$	$0.3 \times 10^1$ *	[71]
HP1:5'-TCTCCGCCGAGAGAGAGATCCAATCACAACCTCTCTCTCGCCGTCTCTC-3'	As <sup>3+</sup>	Fluorescence	$0.1 \times 10^{-3} - 0.1 \times 10^5$	$0.5 \times 10^{-2}$	[72]
5'-ACCGACCGTGCTGGACTCTGGACTGTTGTGG	Cd <sup>2+</sup>	Colorimetric	$0.2 \times 10^1 - 0.2 \times 10^2$	$0.112 \times 10^1$	[63]
5'-SH C <sub>6</sub> -CGGCTTTTGTGTTT-3'	Hg <sup>2+</sup>	MRS	$0.1 \times 10^2 - 0.5 \times 10^4$ *	$0.27 \times 10^1$ *	[73]
5'-FAM-CTCAGTCGACGACGGCCAGTAGCTGACATCAGTGACGATCTAG-TCGTCA	Pb <sup>2+</sup>	Fluorescence	$0.1 \times 10^3 - 0.1 \times 10^4$ *	$0.607 \times 10^2$ *	[74]
5'-Biotin-TTCTTCTTCTTTC-3'	Hg <sup>2+</sup>	Fluorescence	$0.2 \times 10^1 - 0.160 \times 10^3$ *	0.2 *	[75]
HS-(CH <sub>2</sub> ) <sub>6</sub> -TTTTTTTTTTGGGGGGGAAAAA	Hg <sup>2+</sup>	SERS	$0.1 \times 10^2 - 0.1 \times 10^7$ *	-	[76]
5'-GGTTGGTGTGGTGGTTGGT-GTTGG-3'	Pb <sup>2+</sup>	SERS	$0.13 - 0.5333 \times 10^2$ *	0.07 *	[77]
5'-NH <sub>2</sub> -C <sub>6</sub> -GTGGTGGGTGGGTGGGT-3'	Pb <sup>2+</sup>	Optical	$0.5 \times 10^3 - 0.1 \times 10^5$ *	-	[78]
5'-GGGTGGGTGGGTGGGT-C <sub>6</sub> -SH-3'	Pb <sup>2+</sup>	DPV	$0.16 \times 10^{-3} - 0.16$ *	$0.32 \times 10^{-4}$ *	[79]
5'-SH-(CH <sub>2</sub> ) <sub>6</sub> -TTTCATCTTCTCCGAGCCGGTCGAAATAGTGAGT-3'	Pb <sup>2+</sup>	Chronocoulometric	$0.5 \times 10^{-1} - 0.1 \times 10^3$ *	$0.12 \times 10^{-1}$ *	[80]

\* Concentration in (nM).

**Table 3.** Detection of heavy metals using MIP based sensors.

Functional Monomer	Cross Linker	Analyte	Detection Method	Linear Range $\mu\text{g L}^{-1}$	LOD $\mu\text{g L}^{-1}$	Ref.
<b>Chitosan</b> <b>3-(2-aminoethylamino)</b> <b>propyltrimethoxysilane</b>	Epichlorohydrin	$\text{Cu}^{2+}$	DPASV	$0.5 \times 10^3$ – $0.1 \times 10^6$ *	$0.15 \times 10^3$ *	[81]
	and tetra-ethylorthosilicate	$\text{Co}^{2+}$	FAAS	$0.1 \times 10^1$ – $0.13 \times 10^3$	0.15	[82]
<b>methacrylic acid</b> <b>methacrylic acid</b>	ethylene glycol dimethacrylate	$\text{Hg}^{2+}$	SWASV	$0.7 \times 10^{-1}$ – $0.8 \times 10^2$	$0.2 \times 10^{-1}$	[83]
	ethylene glycol dimethacrylate	$\text{Hg}^{2+}$	Potentiometry	$0.4 \times 10^1$ – $0.13 \times 10^7$ *	$0.195 \times 10^1$ *	[84]
<b>polyethylenimine and methacrylic acid</b> <b>acryl amide</b>	ethylene glycol dimethacrylate	$\text{Cd}^{2+}$	Colorimetric	$0.1 \times 10^1$ – $0.1 \times 10^3$	0.4	[63]
	N,N methylenebisacryl amide	$\text{Co}^{2+}$	CSDPV	$0.5$ – $0.5 \times 10^3$ *	0.1 *	[85]
<b>N-[4-(2-Oxo-2H-chromen-3-yl)-</b> <b>thiazol-2-yl]-acrylamide</b>	ethylene glycol dimethacrylate	$\text{Hg}^{2+}$	Fluorescence	$0.5 \times 10^{-1}$ – $0.12 \times 10^1$	$0.2 \times 10^{-1}$	[86]
<b>3-Aminopropyltriethoxysilane</b>	tetramethoxysilane	$\text{Cu}^{2+}$ $\text{Hg}^{2+}$	Fluorescence	$0.11$ – $0.58 \times 10^2$ ( $\text{Cu}^{2+}$ ) $0.26$ – $0.34 \times 10^2$ ( $\text{Hg}^{2+}$ )	$0.35 \times 10^{-1}$ ( $\text{Cu}^{2+}$ ) $0.56$ $\times 10^{-1}$ ( $\text{Hg}^{2+}$ )	[87]
<b>4-vinyl pyridine</b>	ethylene glycol dimethacrylate	$\text{Pb}^{2+}$	DPV	$0.1$ – $0.8 \times 10^2$	$0.5 \times 10^{-1}$	[88]
<b>cetyltrimethylammonium bromide</b>	tetraethylorthosilicate	$\text{Pb}^{2+}$ $\text{Ag}^+$	Fluorescence	$0.5 \times 10^2$ – $0.9 \times 10^3$ * ( $\text{Pb}^{2+}$ ) $0.2 \times 10^3$ – $0.125$ $\times 10^5$ ( $\text{Ag}^+$ )	$0.26 \times 10^2$ * ( $\text{Pb}^{2+}$ ) $0.86$ $\times 10^2$ * ( $\text{Ag}^+$ )	[89]

\* Concentration in (nM).

### 2.3.2. Lead Sensing

Lead is one of the most well-known toxic heavy-metal elements, and chronic exposure can affect the central nervous system, which leads to brain damage in children and kidney damage in infants and children [90]. Therefore, there is an urgent need for the health of human beings to develop a highly sensitive and selective technique for the trace detection of  $Pb^{2+}$  in drinking water. Various electrochemical methods have been used for lead detection, because of the simplification, sensitivity, and cost-effectiveness of these methods. Recently, special recognition elements, like  $Pb^{2+}$ -specific DNAzymes and Pb(II)-IIP, have been employed to further improve the selectivity of electrochemical detection platforms. As an example, Xu et al. [67] developed an electrochemical aptasensor that was based on G-rich lead-specific aptamer (LSA) as the recognition element of  $Pb^{2+}$  and AgPtNPs/MIL-101(Fe) as signal probes and electrocatalytic enhancers for the detection of  $Pb^{2+}$ . The selectivity of the sensor was improved by the special interaction between  $Pb^{2+}$  and G-rich LSA. Additionally, an electrochemical aptasensor for  $Pb^{2+}$  detection was designed using thionine (TH) as the signaling molecule and graphene (GR) as the signal-enhancing platform [79]. Recently, the Dahaghin group [88] fabricated a new IIP, grafted onto  $Fe_3O_4$  NPs, and then applied them as modifiers to design a Pb-selective voltammetric sensor. IIP was synthesized using 2-(2-aminophenyl)-1H-benzimidazole, 4-vinyl pyridine,  $Pb(NO_3)_2$ , ethylene glycol dimethylacrylate, and AIBN as the lead-binding ligand, functional monomers, template, cross-linker, and initiator, respectively. Attaching the IIP on the modified nano-scale magnetic particle led to enhanced adsorption capacity and the relative respective surface area. Fluorescence probes based on fluorescent nanoparticles as a detection method has attracted a lot of attention for lead detection, because of their low background, improved optical properties, and facile chemical functionalization and modification. In this regard, Zhang et al. introduced a turn-on fluorescent biosensor for the selective detection of  $Pb^{2+}$  using C-PS2.M-DNA-templated silver nanoclusters (Ag NCs) [70]. This DNA template consists of two segments: one is the Ag NCs-nucleation segment at the two termini and the other is the aptamer segment of  $Pb^{2+}$  in the middle of DNA template. In the presence of  $Pb^{2+}$  ions, the interaction between  $Pb^{2+}$  and the aptamer leads to a conformational change in the aptamer and causes the two darkish DNA–Ag NCs to aggregate together, resulting in the fluorescence switch-on detection of  $Pb^{2+}$ . Recently, a dual reference ion-imprinted ratiometric fluorescence probe for the simultaneous detection of  $Ag^+$  and  $Pb^{2+}$  was reported [89]. Carbon dots (CDs) and gold nanoclusters (AuNCs) were employed for the fluorescence signal output to monitor  $Ag^+$  and  $Pb^{2+}$ , respectively. Functional groups on the surface of fluorescence nanoparticles were employed to form a chelate with the template ions during the polymerization in order to enhance the conversion efficiency from molecular recognition into a fluorescence signal output.

### 2.3.3. Mercury Sensing

Mercury is present in the inorganic form in surface water and groundwater and its toxic effects are mainly seen in the kidney. The maximum contaminant levels of inorganic mercury is defined as  $6 \mu gL^{-1}$  and  $2 \mu gL^{-1}$  by WHO and EPA, respectively [61,62]. Electrochemical techniques have been widely applied as powerful tools because of their attractive properties, such as simple instrumentation and rapid response. An electrochemical sensor based on RGO–IIP (RGO= reduced graphene oxide) for the selective detection of trace mercury ions in water samples was fabricated by Ghanei-Motlagh's team [83]. They synthesized IIP on the RGO surface as a supporting material through the surface imprinting technique to overcome the problems, which are caused by bulk polymerization methods, such as incomplete template removal and template leakage. Recently, a gold inkjet-printed impedimetric platform for the aptamer-based detection of  $Hg^{2+}$  with high stability under harsh conditions was reported [68]. In this biosensor, once  $Hg^{2+}$  binds selectively to the N3 of thymidine, creating a bridge between two thymidine residues and form a base-pair, the secondary conformation of the poly(T) ssDNA aptamers immobilized on the electrode surface changes into a "hair-pin" like structure.

Fluorescent based assays as another attractive technique have shown promise for mercury detection. As an example, Hande et al. [86] first synthesized fluorescent N-[4-(2-Oxo-2H-chromen-

3-yl)-thiazol-2-yl]-acrylamide (OCTAA) monomers with very good chelating properties as it gets quenched with various metal ions. Subsequently, they applied OCTAA to fabricate a Hg(II)-IIP based fluorescent sensor for the selective detection of mercury. Recently, a fluorescent aptasensor that was based on magnetic separation and the formation of T-Hg<sup>2+</sup>-T base pairs was designed [75]. Aptamer functionalized magnetic beads (AMB) were formed by the immobilization of aptamers on the surface of magnetic beads. It was reported that the fluorescence signal of the detection solution was enhanced in the presence of Hg<sup>2+</sup> ions, because of the release of higher amounts of the signal transduction probe (STP) for the detection solution after magnetic separation. Therefore, the quantitative detection of mercury ions can be achieved by the fluorescence signal intensity of STP. The direct binding of metal ions with the signal probe can effectively eliminate the heavy metal-fluorescence quenching effect, so the sensitivity of the presented sensor improved because of the avoidance of the direct binding of Hg<sup>2+</sup> with STP. Aptasensors and IIP based sensors have both shown comparable performance for the sensitive and selective detection of heavy metals. Besides the sensitivity and selectivity, the regeneration of the sensors is crucial in practical applications [91]. However, despite the high performance of the reported aptasensors towards the detection of heavy metals, only a few of them have incorporated the regeneration of the analyte [79]. In contrast, it seems that the regeneration of IIP based sensors is not a challenging issue, because they could be easily reproduced using the procedure, which has already been employed to remove the template in the IIP synthesis procedure.

#### 2.4. MIPs and Aptamers in the Detection of Large Pathogen Contaminants

Sensitive and rapid detection of environmental pathogens, mainly for virus and bacteria, is important to address the drug resistance issues and prevent the outbreaks of pathogenic diseases from water sources. The most common practices to quantify pathogens are polymerase chain reaction (PCR) and bacteria culture tests [92,93]. However, these methods are complex, require multiple-steps, and are labor intensive with long assay-times (>1 day). The integration of MIPs and aptamers with biosensor devices as the bio-recognition elements for the detection of environmental pathogens (e.g., foodborne and waterborne) has been shown to be flourishing measures, due to their remarkable advances accredited to their excellent recognition specificity, ease of synthesis, low cost, and eco-friendly nature [94–96].

##### 2.4.1. Bacteria Detection

The most frequent waterborne and foodborne bacterial illnesses are caused by *Escherichia coli* (*E. coli*) O157:H7, *Campylobacter* spp., *Legionella* spp., *Giardia*, *Bacillus cereus*, *Cryptosporidium*, *Salmonella* spp., *Yersinia enterocolitica*, *Enterococcus faecalis*, and *Shigella* [97–99]. The development of whole cell imprinted-based sensors is somewhat challenging. Cytosensing based on the cell shape recognition does not always provide an acceptable specificity due to the high degree of cell plasticity to easily undergo morphology changes under small influences. Moreover, the micrometer size of the cells and their three-dimensional features make it difficult to fabricate a very selective and rigid monomer [100]. Therefore, one critical element would be choosing the right monomers for the fabrication of highly selective and specific platforms. For instance, Spieker et al. developed a MIP-based biosensor for the detection of *Bacillus cereus* [101]. They screened the affinity of *Bacillus cereus* on different polymers of polyacrylate (PA), polystyrene (PS), polyacrylamide (PAA), polyvinylpyrrolidone (PVP), and polyurethane (PU), and found that the developed sensor showed a remarkable selectivity and linear response when PU was coated on the quartz crystal microbalance (QCM). The proposed sensor could detect  $9.6 \times 10^7$  cells/mL with a linear response from  $9.6 \times 10^7$  to  $7.7 \times 10^8$  cells/mL. Although a very simple 60 nt aptasensor had already been developed by Ikanovic et al. for the optical detection of *Bacillus thuringiensis* spores as low as  $10^3$  cfu/mL with linear range of  $10^3$ – $10^6$  cfu/mL, using core-shell zinc sulfide cadmium selenide quantum dots (QD) [102]. In another study, four different materials of Poly(vinyl alcohol)/N-methyl-4(4'-formylstyryl)pyridinium methosulfate acetal (PVASbQ), Epon1002F, and polyurethanes with/without 10% OH excess were analyzed for the establishment of *E. coli* surface

imprints. From the atomic force microscopy (AFM) pictures presented in Figure 1, the proper formation of *E. coli* imprints on the commercially available Epon1002F is evident. Additionally, the best sensing performance was attributed to the same material with an LOD of  $1.4 \times 10^7$  cfu/mL and linear detection range of  $7.3\text{--}0.4 \times 10^7$  cfu/mL [103]. On the other hand, recently, a very sensitive fluorescence-based aptasensor was reported for the detection of *E. coli* in pork samples down to 10 cfu/mL and a linear range of  $58\text{--}58 \times 10^6$  cfu/mL [104]. Although the aptasensor was more sensitive, the surface imprint technique was a faster approach and it was based on a commercial resin, making it a more practical approach. Choi et al. and Crapnell and co-workers reviewed more details regarding the monomer types [46,105].

By combination of electrochemistry and optical methods, a more sensitive sandwich assay for the quantification of *E. coli* O157:H7 was developed, while using an electrochemiluminescence (ECL) technique. A polydopamine (PDA) surface imprinted polymer was electropolymerized on the glassy carbon electrode (GCE) in the presence of the target bacteria. After the template removal, sandwich assay was formed by means of nitrogen-doped graphene quantum dot-conjugated antibody to give rise to a linear detection range of 10 to  $10^7$  cfu/mL and detection limit of 8 cfu/mL [106].

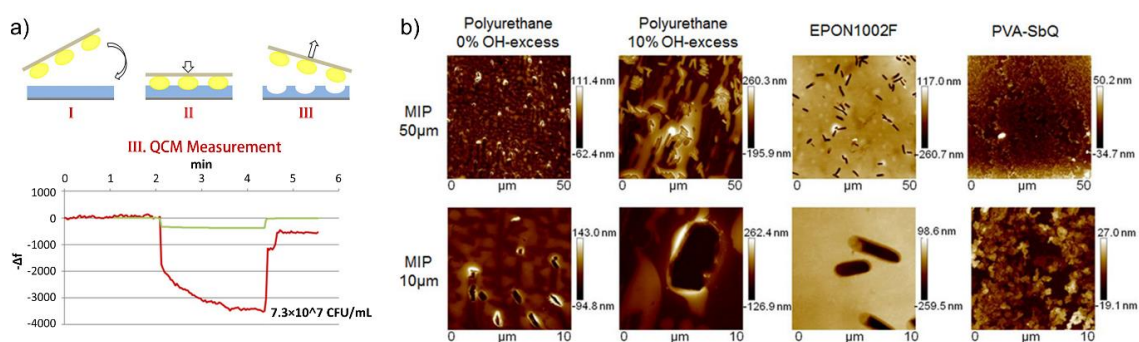


**Figure 1.** (a) Surface imprinting and a typical quartz crystal microbalance (QCM) curve for sensor response upon *E. coli* addition, (b) atomic force microscopy (AFM) pictures of four different imprinted polymers. Reprinted (adapted) with permission from [103]. Copyright (2017) Chemical Society American.

Likewise, Hua and co-workers used aptasensors and photoelectrochemical techniques to detect *E. coli* in milk samples with ultra-sensitivity down to 0.66 cfu/mL and a linear response from 2.9 to  $2.9 \times 10^6$  cfu/mL [107]. The high performance of the fabricated biosensor was attributed to the synergetic role of three-dimensional graphene hydrogel-loaded carbon quantum dots (C-dots/3DGH) and graphene-like carbon nitride (g-C<sub>3</sub>N<sub>4</sub>). Even though both approaches showed ultra-sensitivity, the use of an antibody in the imprinted technique would add cost to the fabrication process, whereas the aptasensor required laborious nanostructure synthesis routes.

The substructure or epitope imprinting approach has been introduced, which involves recognition of particular cell surface components, such as glycomoieties, proteins, lipids, etc., in order to address the challenges of the whole cell imprinting [108]. For example, Saylan et al. have recently reported a novel strategy from which, instead of the whole microorganism, the extracted surface proteins of the bacteria *Enterococcus faecalis* were imprinted on a nanopolymer (Figure 2). They could successfully detect this human fecal contamination in drinking water with an LOD of  $3.4 \times 10^4$  cfu/mL and linear detection range of  $5 \times 10^4\text{--}5 \times 10^8$  cfu/mL [109]. Nonetheless, the method needs more study to increase its sensitivity. To this end, regarding the bacteria detection, aptasensors have shown better performance than those of the imprinted techniques. Although, when compared with aptamers, the higher tailorability of MIPs to be molded as the solid films, particles, nanostructures, etc., together with their greater surface functionalization ability, would lead to inevitable progress in the development of high-throughput MIP-based sensors in the near future.

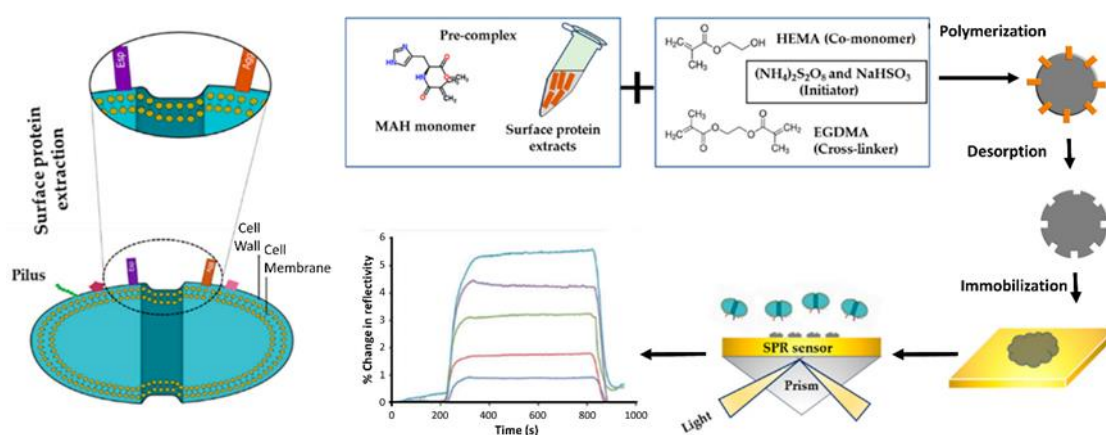


**Figure 2.** Scheme of MIP fabrication and sensing mechanism. Reproduced with the permission from [109].

#### 2.4.2. Virus Detection

Major environmental viruses are known to be hepatitis A and E viruses, norovirus, astrovirus, and rotavirus [97,110]. Virus imprinting has shown very promising outcomes for the diagnosis of virus-associated diseases [38]. However, the application of aptasensors for environmental viruses is still in its infancy despite the flourishing outcomes for virus detection using aptamers [111]. The most studied aptasensors are associated with norovirus, which is the main foodborne virus and the major cause of acute gastroenteritis worldwide [112].

A study by Altintas et al. demonstrated the great capability of a MIP-based plasmonic biosensor to selectively quantify the waterborne bacteriophage-M2 with a high degree of sensitivity [113]. First, MIP nanoparticles were polymerized on the bacteriophage-M2, which was immobilized onto a functionalized glass bead. Subsequently, the imprinted MIP nanoparticles were detached and used for the functionalization of the SPR chips for further target detection. This method provided a good LOD of  $5 \times 10^6$  pfu/mL (converted from the equivalent molarity) and a linear range of 0.33–27 pmol. The proposed sensor also demonstrated a rigid regeneration capability for sequential analysis of the target virus to represent a proper methodology for the detection and purification of water pathogens. Zhang et al. proposed another simple and sensitive method for the immediate detection of hepatitis A virus (HAV) [114]. Virus-magnetic-MIPs were fabricated by self-polymerization of dopamine on magnetic  $\text{Fe}_3\text{O}_4$  nanoparticles in the presence of HAV, as illustrated in Figure 3. Later, the HAV was removed to form the sensor probe. Rebinding the target HAV with magnetic-MIPs was followed by changes in the RLS intensity. The proposed strategy could rectify the difficulties of MIP-based virus detection systems in the elution process. The proposed method has a significant capability to be a universal platform for various types of virus, given its high specificity, low LOD of 6.2 pM, and good linear range of 0.02 nM to 1.4 nM.

On the other hand, in 2013, a DNA aptamer against murine norovirus was synthesized and used for the development of a simple, label-free, and fast electrochemical device to detect norovirus (LOD = 10 aM) in meat juice samples (Figure 4) [115]. The synthesized aptamer (AG3) displayed a high affinity down to the picomolar range for norovirus with a million-fold higher affinity than a morphologically similar virus (feline calicivirus). The fabrication and detection simplicity, low cost, and fast response of the proposed biosensor represents the promising potential of the aptasensors for on-site monitoring of the foodborne viruses. Although, its narrow linear detection range (20 aM to 120 aM) was a restriction to be addressed.

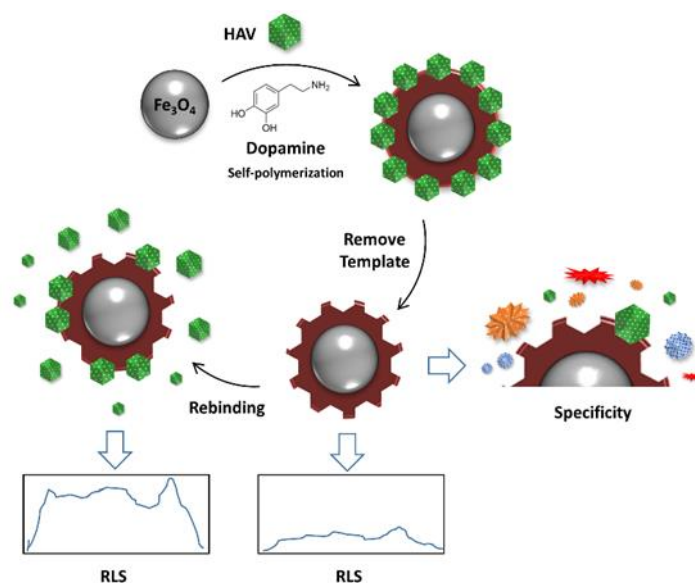


**Figure 3.** Schematic of the virus-magnetic-MIPs assay reproduced from [114].

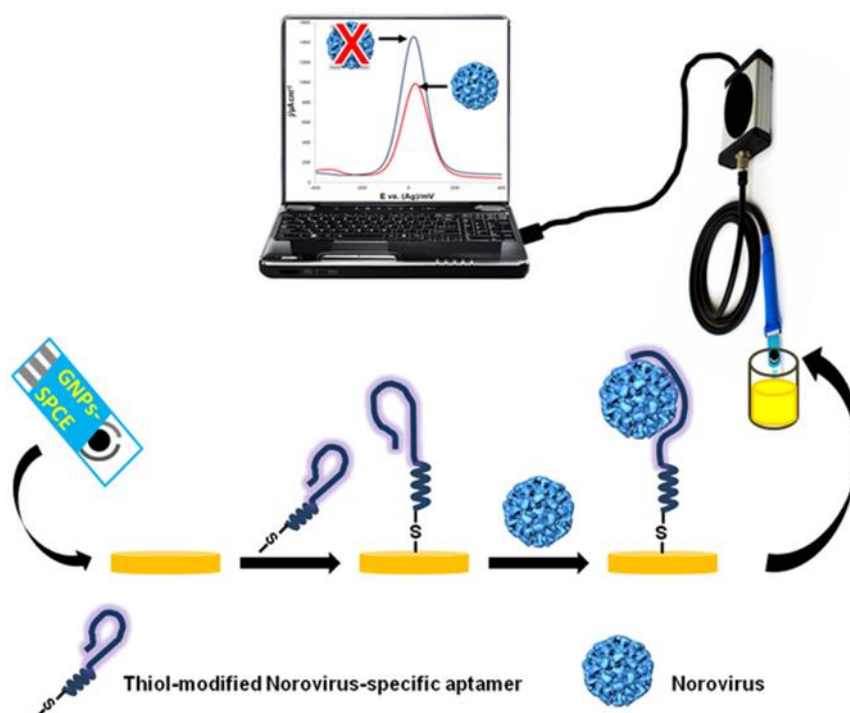


**Figure 4.** Schematic of the aptasensor for electrochemical detection of norovirus. Reproduced with the permission from [115].

In another study, Escudero-Abarca et al. developed another specific DNA aptamer for GII.2 norovirus. Using aptamer magnetic capture (AMC) coupled with RT-qPCR assay, they successfully detected 10 RNA per sample of lettuce [116]. The capture efficiency of the developed aptamers were within the range of 2.5–36% with nanomolar affinities being reported. Later, Kim et al. used the same aptamer that was developed by Escudero-Abarca et al. and fabricated a very sensitive chemiluminescence-based biosensor for the direct quantification of GII.2 norovirus in tap water as low as 80 ng/mL with a linear detection range of between 0.16–10  $\mu\text{g/mL}$  [117]. The developed assay was based on the association/dissociation of the aptamer from the virus capsid and quenching/emission of light in the presence of 3,4,5-trimethoxyphenylglyoxal (TMPG) and tetra-*n*-propylammonium

hydroxide (TPA). The enhanced chemiluminescence was attributed to the five extra guanines at the 5' end of the aptamer. The developed biosensor can be implemented for the analysis of different foodborne pathogens, such as *salmonella*, *vibrio*, and *listeria*.

In spite of the sound performance of the reported aptasensors, they are limited to one environmental virus, which reflects the complex and very difficult procedures of the aptamer selection. In contrast, the capability of MIPs to develop specific bio-recognition elements for numerous virus types can pave the way for the fabrication of various sensors for virus detection in real samples.

### 3. Conclusions and Future Directions

The use of MIPs and aptamers as robust receptors for environmental monitoring has shown promise as a possible replacement for other natural based bio-receptors, such as antibodies and enzymes. The literature has shown comparable growth in the number of publications focusing on the use of MIPs and aptamers in the detection of environmental contaminants, although it is interesting to note that these sensors often show a wide range of detection limits, selectivities, and concentration ranges. This might be due to systematic errors between sensor platforms and labs. Both technologies have demonstrated contrasting benefits and drawbacks when demonstrated in the application as recognition elements for the detection of analytes of different masses. This means that there is currently no perfect receptor for biosensor development. For the aptamers field, there is a need to move away from the selection of unmodified aptamers and focus on the development of modified aptamers, which would increase the repertoire of binding interactions for aptamers. However, the lack of simplified, cost effective selection methods for modified aptamers remains a significant bottleneck and, currently, the use of modified aptamers has been largely limited to the fields of drug therapeutics and biomedical fields. For MIPs, significant challenges remain for the development against larger targets, such as proteins and whole cells, which suffer from a lack of available water-soluble functional monomers while still showing significant non-specific binding and lack of access for large templates to their respective recognition sites. Currently, epitope based imprinting and solid phase imprinting have shown great potential as methods for synthesizing MIPs for pathogens. The lack of large-scale commercial development has been the biggest single drawback of both MIPs and aptamers in the last decade. Nevertheless, this is slowly changing with the increase in the number of companies that offer MIPs and aptamers. If we are to see the widespread adoption of these two technologies in this area, then, in general, we need to have at our disposal new simplified methods to develop both these types of technology to see their further commercialization and the eventual replacement of animal derived antibodies.

**Author Contributions:** M.M., M.N., and J.A. wrote the manuscript. Y.S. edited the manuscript. All authors have read and agreed to the published version of the manuscript.

**Funding:** This research was funded by VILLUM FONDEN, grant number (00022912) and Innovation Fund Denmark (IFD), grant number (8127-00021B).

**Conflicts of Interest:** The authors declare no conflict of interest.

### References

1. Rebek, J. Introduction to the Molecular Recognition and Self-Assembly Special Feature. *Proc. Natl. Acad. Sci. USA* **2009**, *106*, 10423–10424. [[CrossRef](#)]
2. Vater, A.; Klusmann, S. Turning mirror-image oligonucleotides into drugs: The evolution of Spiegelmer<sup>®</sup> therapeutics. *Drug Discov. Today* **2015**, *20*, 147–155. [[CrossRef](#)]
3. Gawande, B.N.; Rohloff, J.C.; Carter, J.D.; Von Carlowitz, I.; Zhang, C.; Schneider, D.J.; Janjic, N. Selection of DNA aptamers with two modified bases. *Proc. Natl. Acad. Sci. USA* **2017**, *114*, 2898–2903. [[CrossRef](#)]
4. Ni, S.; Yao, H.; Wang, L.; Lu, J.; Jiang, F.; Lu, A.; Zhang, G. Chemical modifications of nucleic acid aptamers for therapeutic purposes. *Int. J. Mol. Sci.* **2017**, *18*, 1683. [[CrossRef](#)]
5. Wang, R.E.; Wu, H.; Niu, Y.; Cai, J. Improving the Stability of Aptamers by Chemical Modification. *Curr. Med. Chem.* **2011**, *18*, 4126–4138. [[CrossRef](#)]

6. Zulkefli, N.S.; Kim, K.H.; Hwang, S.J. Effects of microbial activity and environmental parameters on the degradation of extracellular environmental DNA from a eutrophic lake. *Int. J. Environ. Res. Public Health* **2019**, *16*, 3339. [[CrossRef](#)]
7. Chen, L.; Wang, X.; Lu, W.; Wu, X.; Li, J. Molecular imprinting: Perspectives and applications. *Chem. Soc. Rev.* **2016**, *45*, 2137–2211. [[CrossRef](#)]
8. Silvestri, D.; Barbani, N.; Cristallini, C.; Giusti, P.; Ciardelli, G. Molecularly imprinted membranes for an improved recognition of biomolecules in aqueous medium. *J. Memb. Sci.* **2006**, *282*, 284–295. [[CrossRef](#)]
9. Wackerlig, J.; Schirhagl, R. Applications of Molecularly Imprinted Polymer Nanoparticles and Their Advances toward Industrial Use: A Review. *Anal. Chem.* **2016**, *88*, 250–261. [[CrossRef](#)]
10. Poma, A.; Guerreiro, A.; Whitcombe, M.J.; Elena, V. Solid-Phase Synthesis of Molecularly Imprinted Polymer Nanoparticles with a Reusable Template—“Plastic Antibodies”. **2016**, *23*, 2821–2827. [[CrossRef](#)]
11. Ellington, A.D.; Szostak, J.W. In Vitro selection of RNA molecules that bind specific ligands. *Nature* **1990**, *346*, 818–822. [[CrossRef](#)] [[PubMed](#)]
12. Hashim, S.N.N.S.; Boysen, R.I.; Schwarz, L.J.; Danylec, B.; Hearn, M.T.W. A comparison of covalent and non-covalent imprinting strategies for the synthesis of stigmasterol imprinted polymers. *J. Chromatogr. A* **2014**, *1359*, 35–43. [[CrossRef](#)] [[PubMed](#)]
13. Schmidt, R.H.; Haupt, K. Molecularly imprinted polymer films with binding properties enhanced by the reaction-induced phase separation of a sacrificial polymeric porogen. *Chem. Mater.* **2005**, *17*, 1007–1016. [[CrossRef](#)]
14. Ashley, J.; Feng, X.; Halder, A.; Zhou, T.; Sun, Y. Dispersive solid-phase imprinting of proteins for the production of plastic antibodies. *Chem. Commun.* **2018**, *54*, 3355–3358. [[CrossRef](#)]
15. Ashley, J.; Feng, X.T.; Sun, Y. A multifunctional molecularly imprinted polymer-based biosensor for direct detection of doxycycline in food samples. *Talanta* **2018**, *182*, 49–54. [[CrossRef](#)]
16. Zhou, T.; Ashley, J.; Feng, X.; Sun, Y. Detection of hemoglobin using hybrid molecularly imprinted polymers/carbon quantum dots-based nanobiosensor prepared from surfactant-free Pickering emulsion. *Talanta* **2018**, *190*, 443–449. [[CrossRef](#)]
17. Xia, Q.; Yun, Y.; Li, Q.; Huang, Z.; Liang, Z. Preparation and characterization of monodisperse molecularly imprinted polymer microspheres by precipitation polymerization for kaempferol. *Des. Monomers Polym.* **2017**, *20*, 201–209. [[CrossRef](#)]
18. Canfarotta, F.; Poma, A.; Guerreiro, A.; Piletsky, S. Solid-phase synthesis of molecularly imprinted nanoparticles. *Nat. Protoc.* **2016**, *11*, 443–455. [[CrossRef](#)]
19. Yang, K.; Li, S.; Liu, L.; Chen, Y.; Zhou, W.; Pei, J.; Liang, Z.; Zhang, L.; Zhang, Y. Epitope Imprinting Technology: Progress, Applications, and Perspectives toward Artificial Antibodies. *Adv. Mater.* **2019**, *31*, 1–17. [[CrossRef](#)]
20. Altintas, Z.; Takiden, A.; Utesch, T.; Mroginski, M.A.; Schmid, B.; Scheller, F.W.; Süßmuth, R.D. Integrated Approaches Toward High-Affinity Artificial Protein Binders Obtained via Computationally Simulated Epitopes for Protein Recognition. *Adv. Funct. Mater.* **2019**, *29*, 1–11. [[CrossRef](#)]
21. Ashley, J.; Shukor, Y.; Tothill, I.E. The use of differential scanning fluorimetry in the rational design of plastic antibodies for protein targets. *Analyst* **2016**, *141*, 6463–6470. [[CrossRef](#)] [[PubMed](#)]
22. Kalra, P.; Dhiman, A.; Cho, W.C.; Bruno, J.G.; Sharma, T.K. Simple Methods and Rational Design for Enhancing Aptamer Sensitivity and Specificity. *Front. Mol. Biosci.* **2018**, *5*, 41. [[CrossRef](#)] [[PubMed](#)]
23. Ali, M.H.; Elsherbiny, M.E.; Emara, M. Updates on aptamer research. *Int. J. Mol. Sci.* **2019**, *20*, 2511. [[CrossRef](#)]
24. Kaur, H.; Bruno, J.G.; Kumar, A.; Sharma, T.K. Aptamers in the therapeutics and diagnostics pipelines. *Theranostics* **2018**, *8*, 4016–4032. [[CrossRef](#)]
25. Lu, W.; Xue, M.; Xu, Z.; Dong, X.; Xue, F.; Wang, F.; Wang, Q.; Meng, Z. Molecularly imprinted polymers for the sensing of explosives and chemical warfare agents. *Curr. Org. Chem.* **2015**, *19*, 62–71. [[CrossRef](#)]
26. Whitcombe, M.J.; Chianella, I.; Larcombe, L.; Piletsky, S.A.; Noble, J.; Porter, R.; Horgan, A. The rational development of molecularly imprinted polymer-based sensors for protein detection. *Chem. Soc. Rev.* **2011**, *40*, 1547–1571. [[CrossRef](#)]
27. Martin, J.A.; Smith, J.E.; Warren, M.; Chávez, J.L.; Hagen, J.A.; Kelley-Loughnane, N. A Method for Selecting Structure-switching Aptamers Applied to a Colorimetric Gold Nanoparticle Assay. *J. Vis. Exp.* **2015**, *96*, e52545. [[CrossRef](#)]

28. McKeague, M.; Derosa, M.C. Challenges and opportunities for small molecule aptamer development. *J. Nucleic Acids* **2012**, *2012*, 20. [[CrossRef](#)]
29. Rangel, A.E.; Chen, Z.; Ayele, T.M.; Heemstra, J.M. In Vitro selection of an XNA aptamer capable of small-molecule recognition. *Nucleic Acids Res.* **2018**, *46*, 8057–8068. [[CrossRef](#)]
30. Thiel, W.H.; Bair, T.; Wyatt Thiel, K.; Dassie, J.P.; Rockey, W.M.; Howell, C.A.; Liu, X.Y.; Dupuy, A.J.; Huang, L.; Owczarzy, R.; et al. Nucleotide bias observed with a short SELEX RNA aptamer library. *Nucleic Acid Ther.* **2011**, *21*, 253–263. [[CrossRef](#)]
31. Berezovski, M.; Musheev, M.; Drabovich, A.; Krylov, S.N. Non-SELEX Selection of Aptamers. *J. Am. Chem. Soc.* **2006**, *128*, 1410–1411. [[CrossRef](#)] [[PubMed](#)]
32. Nishimura, K.; Haginaka, J. Preparation and evaluation of molecularly imprinted polymers for promazine and chlorpromazine by multi-step swelling and polymerization: The application for the determination of promazine in rat serum by column-switching LC. *Anal. Sci.* **2019**, *35*, 659–664. [[CrossRef](#)] [[PubMed](#)]
33. Larpant, N.; Suwanwong, Y.; Boonpangrak, S.; Laiwattanapaisal, W. Exploring matrix effects on binding properties and characterization of cotinine molecularly imprinted polymer on paper-based scaffold. *Polymers* **2019**, *11*, 570. [[CrossRef](#)] [[PubMed](#)]
34. Madikizela, L.M.; Tavengwa, N.T.; Tutu, H.; Chimuka, L. Green aspects in molecular imprinting technology: From design to environmental applications. *Trends Environ. Anal. Chem.* **2018**, *17*, 14–22. [[CrossRef](#)]
35. El-Sharif, H.F.; Hawkins, D.M.; Stevenson, D.; Reddy, S.M. Determination of protein binding affinities within hydrogel-based molecularly imprinted polymers (HydroMIPs). *Phys. Chem. Chem. Phys.* **2014**, *16*, 15483–15489. [[CrossRef](#)]
36. Rampey, A.M.; Umpleby, R.J.; Rushton, G.T.; Iseman, J.C.; Shah, R.N.; Shimizu, K.D. Characterization of the Imprint Effect and the Influence of Imprinting Conditions on Affinity, Capacity, and Heterogeneity in Molecularly Imprinted Polymers Using the Freundlich Isotherm-Affinity Distribution Analysis. *Anal. Chem.* **2004**, *76*, 1123–1133. [[CrossRef](#)]
37. Jing, M.; Bowser, M.T. Methods for measuring aptamer-protein equilibria: A review. *Anal. Chim. Acta* **2011**, *686*, 9–18. [[CrossRef](#)]
38. Gast, M.; Sobek, H.; Mizaikoff, B. Advances in imprinting strategies for selective virus recognition a review. *TrAC Trends Anal. Chem.* **2019**, *114*, 218–232. [[CrossRef](#)]
39. Verheyen, E.; Schillemans, J.P.; Van Wijk, M.; Demeniex, M.A.; Hennink, W.E.; Van Nostrum, C.F. Challenges for the effective molecular imprinting of proteins. *Biomaterials* **2011**, *32*, 3008–3020. [[CrossRef](#)]
40. Ohuchi, S. Cell-Selex technology. *Biores. Open Access* **2012**, *1*, 265–272. [[CrossRef](#)]
41. Song, X.; Wang, J.; Zhu, J. Effect of porogenic solvent on selective performance of molecularly imprinted polymer for quercetin. *Mater. Res.* **2009**, *12*, 299–304. [[CrossRef](#)]
42. Busato, M.; Distefano, R.; Bates, F.; Karim, K.; Bossi, A.M.; López Vilariño, J.M.; Piletsky, S.; Bombieri, N.; Giorgetti, A. MIRATE: MIPs RAtional dESign Science Gateway. *J. Integr. Bioinform.* **2018**, *15*, 1–6. [[CrossRef](#)] [[PubMed](#)]
43. Ciardelli, G.; Silvestri, D.; Cristallini, C.; Barbani, N.; Giusti, P. The relevance of the transfer of molecular information between natural and synthetic materials in the realisation of biomedical devices with enhanced properties. *J. Biomater. Sci. Polym. Ed.* **2005**, *16*, 219–236. [[CrossRef](#)] [[PubMed](#)]
44. Poma, A.; Brahmabhatt, H.; Pendergraft, H.M.; Watts, J.K.; Turner, N.W. Generation of novel hybrid aptamer-molecularly imprinted polymeric nanoparticles. *Adv. Mater.* **2015**, *27*, 750–758. [[CrossRef](#)]
45. Odeh, F.; Nsairat, H.; Alshaer, W.; Ismail, M.A.; Esawi, E.; Qaqish, B.; Bawab, A.A.; Ismail, S.I. Aptamers chemistry: Chemical modifications and conjugation strategies. *Molecules* **2020**, *25*, 3. [[CrossRef](#)]
46. Crapnell, R.D.; Hudson, A.; Foster, C.W.; Eersels, K.; van Grinsven, B.; Cleij, T.J.; Banks, C.E.; Peeters, M. Recent advances in electrosynthesized molecularly imprinted polymer sensing platforms for bioanalyte detection. *Sensors* **2019**, *19*, 1204. [[CrossRef](#)]
47. Kamra, T.; Chaudhary, S.; Xu, C.; Johansson, N.; Montelius, L.; Schnadt, J.; Ye, L. Covalent immobilization of molecularly imprinted polymer nanoparticles using an epoxy silane. *J. Colloid Interface Sci.* **2015**, *445*, 277–284. [[CrossRef](#)]
48. Smolinska-Kempisty, K.; Guerreiro, A.; Canfarotta, F.; Cáceres, C.; Whitcombe, M.J.; Piletsky, S. A comparison of the performance of molecularly imprinted polymer nanoparticles for small molecule targets and antibodies in the ELISA format. *Sci. Rep.* **2016**, *6*, 1–7. [[CrossRef](#)]

49. Dong, J.; Li, H.; Yan, P.; Xu, L.; Zhang, J.; Qian, J.; Chen, J.; Li, H. A label-free photoelectrochemical aptasensor for tetracycline based on Au/BiOI composites. *Inorg. Chem. Commun.* **2019**, *109*, 107557. [[CrossRef](#)]
50. Clarindo, J.E.S.; Viana, R.B.; Cervini, P.; Silva, A.B.F.; Cavalheiro, E.T.G. Determination of Tetracycline Using a Graphite-Polyurethane Composite Electrode Modified with a Molecularly Imprinted Polymer. *Anal. Lett.* **2020**, 1–24. [[CrossRef](#)]
51. Zhang, L.; Chen, L. Fluorescence Probe Based on Hybrid Mesoporous Silica/Quantum Dot/Molecularly Imprinted Polymer for Detection of Tetracycline. *ACS Appl. Mater. Interfaces* **2016**, *8*, 16248–16256. [[CrossRef](#)] [[PubMed](#)]
52. Jalalian, S.H.; Taghdisi, S.M.; Danesh, N.M.; Bakhtiari, H.; Lavaee, P.; Ramezani, M.; Abnous, K. Sensitive and fast detection of tetracycline using an aptasensor. *Anal. Methods* **2015**, *7*, 2523–2528. [[CrossRef](#)]
53. Jamieson, O.; Soares, T.C.C.; de Faria, B.A.; Hudson, A.; Mecozzi, F.; Rowley-Neale, S.J.; Banks, C.E.; Gruber, J.; Novakovic, K.; Peeters, M.; et al. Screen printed electrode based detection systems for the antibiotic amoxicillin in aqueous samples utilising molecularly imprinted polymers as synthetic receptors. *Chemosensors* **2020**, *8*, 5. [[CrossRef](#)]
54. Youn, H.; Lee, K.; Her, J.; Jeon, J.; Mok, J.; So, J.I.; Shin, S.; Ban, C. Aptasensor for multiplex detection of antibiotics based on FRET strategy combined with aptamer/graphene oxide complex. *Sci. Rep.* **2019**, *9*, 1–9. [[CrossRef](#)] [[PubMed](#)]
55. Geng, Y.; Guo, M.; Tan, J.; Huang, S.; Tang, Y.; Tan, L.; Liang, Y. A fluorescent molecularly imprinted polymer using aptamer as a functional monomer for sensing of kanamycin. *Sens. Actuators B Chem.* **2018**, *268*, 47–54. [[CrossRef](#)]
56. Székács, A.; Mörtl, M.; Darvas, B. Monitoring pesticide residues in surface and ground water in Hungary: Surveys in 1990–2015. *J. Chem.* **2015**, *2015*, 15. [[CrossRef](#)]
57. Liu, M.; Khan, A.; Wang, Z.; Liu, Y.; Yang, G.; Deng, Y.; He, N. Aptasensors for pesticide detection. *Biosens. Bioelectron.* **2019**, *130*, 174–184. [[CrossRef](#)]
58. Farooq, S.; Nie, J.; Cheng, Y.; Yan, Z.; Li, J.; Bacha, S.A.S.; Mushtaq, A.; Zhang, H. Molecularly imprinted polymers' application in pesticide residue detection. *Analyst* **2018**, *143*, 3971–3989. [[CrossRef](#)]
59. Weerathunge, P.; Behera, B.K.; Zihara, S.; Singh, M.; Prasad, S.N.; Hashmi, S.; Mariathomas, P.R.D.; Bansal, V.; Ramanathan, R. Dynamic interactions between peroxidase-mimic silver NanoZymes and chlorpyrifos-specific aptamers enable highly-specific pesticide sensing in river water. *Anal. Chim. Acta* **2019**, *1083*, 157–165. [[CrossRef](#)]
60. Huang, W.; Zhou, X.; Luan, Y.; Cao, Y.; Wang, N.; Lu, Y.; Liu, T.; Xu, W. A sensitive electrochemical sensor modified with multi-walled carbon nanotubes doped molecularly imprinted silica nanospheres for detecting chlorpyrifos. *J. Sep. Sci.* **2020**, *43*, 954–961. [[CrossRef](#)]
61. Us Epa, O. National primary drinking water regulations: Long Term 1 Enhanced Surface Water Treatment Rule. Final rule. *Fed. Regist.* **2002**, *67*, 1811–1844.
62. Herschy, R.W. *Water Quality for Drinking: WHO Guidelines*; Springer: Berlin/Heidelberg, Germany, 2012; pp. 876–883.
63. Huang, K.; Chen, Y.; Zhou, F.; Zhao, X.; Liu, J.; Mei, S.; Zhou, Y.; Jing, T. Integrated ion imprinted polymers-paper composites for selective and sensitive detection of Cd(II) ions. *J. Hazard. Mater.* **2017**, *333*, 137–143. [[CrossRef](#)] [[PubMed](#)]
64. Zhou, B.; Yang, X.Y.; Wang, Y.S.; Yi, J.C.; Zeng, Z.; Zhang, H.; Chen, Y.T.; Hu, X.J.; Suo, Q.L. Label-free fluorescent aptasensor of Cd<sup>2+</sup> detection based on the conformational switching of aptamer probe and SYBR green I. *Microchem. J.* **2019**, *144*, 377–382. [[CrossRef](#)]
65. Liu, C.W.; Tsai, T.C.; Osawa, M.; Chang, H.C.; Yang, R.J. Aptamer-based sensor for quantitative detection of mercury (II) ions by attenuated total reflection surface enhanced infrared absorption spectroscopy. *Anal. Chim. Acta* **2018**, *1033*, 137–147. [[CrossRef](#)]
66. Khoshbin, Z.; Housaindokht, M.R.; Izadyar, M.; Verdian, A.; Bozorgmehr, M.R. A simple paper-based aptasensor for ultrasensitive detection of lead (II)ion. *Anal. Chim. Acta* **2019**, *1071*, 70–77. [[CrossRef](#)]
67. Xu, W.; Zhou, X.; Gao, J.; Xue, S.; Zhao, J. Label-free and enzyme-free strategy for sensitive electrochemical lead aptasensor by using metal-organic frameworks loaded with AgPt nanoparticles as signal probes and electrocatalytic enhancers. *Electrochim. Acta* **2017**, *251*, 25–31. [[CrossRef](#)]
68. Diaz-Amaya, S.; Lin, L.K.; DiNino, R.E.; Ostos, C.; Stanciu, L.A. Inkjet printed electrochemical aptasensor for detection of Hg<sup>2+</sup> in organic solvents. *Electrochim. Acta* **2019**, *316*, 33–42. [[CrossRef](#)]

69. Wang, H.; Cheng, H.; Wang, J.; Xu, L.; Chen, H.; Pei, R. Selection and characterization of DNA aptamers for the development of light-up biosensor to detect Cd(II). *Talanta* **2016**, *154*, 498–503. [[CrossRef](#)]
70. Zhang, B.; Wei, C. Highly sensitive and selective detection of Pb<sup>2+</sup> using a turn-on fluorescent aptamer DNA silver nanoclusters sensor. *Talanta* **2018**, *182*, 125–130. [[CrossRef](#)]
71. Pan, J.; Li, Q.; Zhou, D.; Chen, J. Ultrasensitive aptamer biosensor for arsenic (III) detection based on label-free triple-helix molecular switch and fluorescence sensing platform. *Talanta* **2018**, *189*, 370–376. [[CrossRef](#)]
72. Gan, Y.; Liang, T.; Hu, Q.; Zhong, L.; Wang, X.; Wan, H.; Wang, P. In-situ detection of cadmium with aptamer functionalized gold nanoparticles based on smartphone-based colorimetric system. *Talanta* **2020**, *208*, 120231. [[CrossRef](#)]
73. Liu, Y.; Cai, Z.; Sheng, L.; Ma, M.; Wang, X. A magnetic relaxation switching and visual dual-mode sensor for selective detection of Hg<sup>2+</sup> based on aptamers modified Au@Fe<sub>3</sub>O<sub>4</sub> nanoparticles. *J. Hazard. Mater.* **2019**, *388*, 121728. [[CrossRef](#)] [[PubMed](#)]
74. Chen, Y.; Li, H.; Gao, T.; Zhang, T.; Xu, L.; Wang, B.; Wang, J.; Pei, R. Selection of DNA aptamers for the development of light-up biosensor to detect Pb(II). *Sens. Actuators B Chem.* **2018**, *254*, 214–221. [[CrossRef](#)]
75. Sun, C.; Sun, R.; Chen, Y.; Tong, Y.; Zhu, J.; Bai, H.; Zhang, S.; Zheng, H.; Ye, H. Utilization of aptamer-functionalized magnetic beads for highly accurate fluorescent detection of mercury (II) in environment and food. *Sens. Actuators B Chem.* **2018**, *255*, 775–780. [[CrossRef](#)]
76. Lu, Y.; Zhong, J.; Yao, G.; Huang, Q. A label-free SERS approach to quantitative and selective detection of mercury (II) based on DNA aptamer-modified SiO<sub>2</sub>@Au core/shell nanoparticles. *Sens. Actuators B Chem.* **2018**, *258*, 365–372. [[CrossRef](#)]
77. Ouyang, H.; Ling, S.; Liang, A.; Jiang, Z. A facile aptamer-regulating gold nanoplasmonic SERS detection strategy for trace lead ions. *Sens. Actuators B Chem.* **2018**, *258*, 739–744. [[CrossRef](#)]
78. Ma, L.H.; Wang, H.B.; Fang, B.Y.; Tan, F.; Cao, Y.C.; Zhao, Y. Di Visual detection of trace lead ion based on aptamer and silver staining nano-metal composite. *Colloids Surf. B Biointerfaces* **2018**, *162*, 415–419. [[CrossRef](#)]
79. Gao, F.; Gao, C.; He, S.; Wang, Q.; Wu, A. Label-free electrochemical lead (II) aptasensor using thionine as the signaling molecule and graphene as signal-enhancing platform. *Biosens. Bioelectron.* **2016**, *81*, 15–22. [[CrossRef](#)]
80. Zhang, C.; Lai, C.; Zeng, G.; Huang, D.; Tang, L.; Yang, C.; Zhou, Y.; Qin, L.; Cheng, M. Nanoporous Au-based chronocoulometric aptasensor for amplified detection of Pb<sup>2+</sup> using DNAzyme modified with Au nanoparticles. *Biosens. Bioelectron.* **2016**, *81*, 61–67. [[CrossRef](#)]
81. Wei, P.; Zhu, Z.; Song, R.; Li, Z.; Chen, C. An ion-imprinted sensor based on chitosan-graphene oxide composite polymer modified glassy carbon electrode for environmental sensing application. *Electrochim. Acta* **2019**, *317*, 93–101. [[CrossRef](#)]
82. Khoddami, N.; Shemirani, F. A new magnetic ion-imprinted polymer as a highly selective sorbent for determination of cobalt in biological and environmental samples. *Talanta* **2016**, *146*, 244–252. [[CrossRef](#)] [[PubMed](#)]
83. Ghanei-Motlagh, M.; Taher, M.A.; Heydari, A.; Ghanei-Motlagh, R.; Gupta, V.K. A novel voltammetric sensor for sensitive detection of mercury(II) ions using glassy carbon electrode modified with graphene-based ion imprinted polymer. *Mater. Sci. Eng. C* **2016**, *63*, 367–375. [[CrossRef](#)] [[PubMed](#)]
84. Shirzadmehr, A.; Afkhami, A.; Madrakian, T. A new nano-composite potentiometric sensor containing an Hg<sup>2+</sup>-ion imprinted polymer for the trace determination of mercury ions in different matrices. *J. Mol. Liq.* **2015**, *204*, 227–235. [[CrossRef](#)]
85. Torkashvand, M.; Gholivand, M.B.; Azizi, R. Synthesis, characterization and application of a novel ion-imprinted polymer based voltammetric sensor for selective extraction and trace determination of cobalt (II) ions. *Sens. Actuators B Chem.* **2017**, *243*, 283–291. [[CrossRef](#)]
86. Hande, P.E.; Samui, A.B.; Kulkarni, P.S. Selective nanomolar detection of mercury using coumarin based fluorescent Hg(II)—Ion imprinted polymer. *Sens. Actuators B Chem.* **2017**, *246*, 597–605. [[CrossRef](#)]
87. Qi, J.; Li, B.; Wang, X.; Zhang, Z.; Wang, Z.; Han, J.; Chen, L. Three-dimensional paper-based microfluidic chip device for multiplexed fluorescence detection of Cu<sup>2+</sup> and Hg<sup>2+</sup> ions based on ion imprinting technology. *Sens. Actuators B Chem.* **2017**, *251*, 224–233. [[CrossRef](#)]
88. Dahaghin, Z.; Kilmartin, P.A.; Mousavi, H.Z. Novel ion imprinted polymer electrochemical sensor for the selective detection of lead(II). *Food Chem.* **2020**, *303*, 125374. [[CrossRef](#)]

89. Lu, H.; Yu, C.; Xu, S. A dual reference ion-imprinted ratiometric fluorescence probe for simultaneous detection of silver (I) and lead (II). *Sens. Actuators B Chem.* **2019**, *288*, 691–698. [[CrossRef](#)]
90. Johnson, F.M. The genetic effects of environmental lead. *Mutat. Res. Rev. Mutat. Res.* **1998**, *410*, 123–140. [[CrossRef](#)]
91. Arugula, M.A.; Simonian, A. Novel trends in affinity biosensors: Current challenges and perspectives. *Meas. Sci. Technol.* **2014**, *25*, 032001. [[CrossRef](#)]
92. Skottrup, P.D.; Nicolaisen, M.; Justesen, A.F. Towards on-site pathogen detection using antibody-based sensors. *Biosens. Bioelectron.* **2008**, *24*, 339–348. [[CrossRef](#)]
93. Parra, E.; Segura, F.; Tijero, J.; Pons, I.; Noguera, M.M. Development of a real-time PCR for Bartonella spp. detection, a current emerging microorganism. *Mol. Cell. Probes* **2017**, *32*, 55–59. [[CrossRef](#)] [[PubMed](#)]
94. Cui, F.; Zhou, Z.; Zhou, H.S. Molecularly imprinted polymers and surface imprinted polymers based electrochemical biosensor for infectious diseases. *Sensors* **2020**, *20*, 996. [[CrossRef](#)] [[PubMed](#)]
95. Srivastava, K.R.; Awasthi, S.; Mishra, P.K.; Srivastava, P.K. *Biosensors/Molecular Tools for Detection of Waterborne Pathogens*; Elsevier: Amsterdam, The Netherlands, 2020; ISBN 9780128187838.
96. Yadav, G.S.; Kumar, V.; Aggarwal, N.K. (Eds.) *Aptamers*; Springer: Singapore, 2019; ISBN 978-981-13-8835-4.
97. Bintsis, T. Foodborne pathogens. *AIMS Microbiol.* **2017**, *3*, 529–563. [[CrossRef](#)]
98. Craun, M.F.; Craun, G.F.; Calderon, R.L.; Beach, M.J. Waterborne outbreaks reported in the United States. *J. Water Health* **2006**, *4*, 19–30. [[CrossRef](#)]
99. Scallan, E.; Hoekstra, R.M.; Angulo, F.J.; Tauxe, R.V.; Widdowson, M.A.; Roy, S.L.; Jones, J.L.; Griffin, P.M. Foodborne illness acquired in the United States—Major pathogens. *Emerg. Infect. Dis.* **2011**, *17*, 7–15. [[CrossRef](#)]
100. Gawlitza, K.; Wan, W.; Wagner, S.; Rurack, K. Fluorescent Molecularly Imprinted Polymers. *Adv. Mol. Impr. Mater.* **2016**, 89–128.
101. Spieker, E.; Lieberzeit, P.A. Molecular Imprinting Studies for Developing QCM-sensors for Bacillus Cereus. *Procedia Eng.* **2016**, *168*, 561–564. [[CrossRef](#)]
102. Ikanovic, M.; Rudzinski, W.E.; Bruno, J.G.; Allman, A.; Carrillo, M.P.; Dwarakanath, S.; Bhahdigadi, S.; Rao, P.; Kiel, J.L.; Andrews, C.J. Fluorescence Assay Based on Aptamer-Quantum Dot Binding to Bacillus thuringiensis Spores. *J. Fluoresc.* **2007**, *17*, 193–199. [[CrossRef](#)]
103. Poller, A.-M.; Spieker, E.; Lieberzeit, P.A.; Preininger, C. Surface Imprints: Advantageous Application of Ready2use Materials for Bacterial Quartz-Crystal Microbalance Sensors. *ACS Appl. Mater. Interfaces* **2017**, *9*, 1129–1135. [[CrossRef](#)]
104. Li, H.; Ahmad, W.; Rong, Y.; Chen, Q.; Zuo, M.; Ouyang, Q.; Guo, Z. Designing an aptamer based magnetic and upconversion nanoparticles conjugated fluorescence sensor for screening Escherichia coli in food. *Food Control* **2020**, *107*, 106761. [[CrossRef](#)]
105. Choi, J.R.; Yong, K.W.; Choi, J.Y.; Cowie, A.C. Progress in molecularly imprinted polymers for biomedical applications. *Comb. Chem. High Throughput Screen.* **2019**, *22*, 78–88. [[CrossRef](#)] [[PubMed](#)]
106. Chen, S.; Chen, X.; Zhang, L.; Gao, J.; Ma, Q. Electrochemiluminescence Detection of Escherichia coli O157:H7 Based on a Novel Polydopamine Surface Imprinted Polymer Biosensor. *ACS Appl. Mater. Interfaces* **2017**, *9*, 5430–5436. [[CrossRef](#)] [[PubMed](#)]
107. Hua, R.; Hao, N.; Lu, J.; Qian, J.; Liu, Q.; Li, H.; Wang, K. A sensitive Potentiometric resolved ratiometric Photoelectrochemical aptasensor for Escherichia coli detection fabricated with non-metallic nanomaterials. *Biosens. Bioelectron.* **2018**, *106*, 57–63. [[CrossRef](#)]
108. Piletsky, S.; Canfarotta, F.; Poma, A.; Bossi, A.M.; Piletsky, S. Molecularly Imprinted Polymers for Cell Recognition. *Trends Biotechnol.* **2020**, *38*, 368–387. [[CrossRef](#)]
109. Saylan, Y.; Erdem, Ö.; Cihangir, N.; Denizli, A. Denizli Detecting Fingerprints of Waterborne Bacteria on a Sensor. *Chemosensors* **2019**, *7*, 33. [[CrossRef](#)]
110. Gall, A.M.; Mariñas, B.J.; Lu, Y.; Shisler, J.L. Waterborne Viruses: A Barrier to Safe Drinking Water. *PLoS Pathog.* **2015**, *11*, 1–7. [[CrossRef](#)]
111. Zou, X.; Wu, J.; Gu, J.; Shen, L.; Mao, L. Application of Aptamers in Virus Detection and Antiviral Therapy. *Front. Microbiol.* **2019**, *10*, 1462. [[CrossRef](#)]
112. Glass, R.I.; Parashar, U.D.; Estes, M.K. Norovirus gastroenteritis. *N. Engl. J. Med.* **2009**, *361*, 1776–1785. [[CrossRef](#)]

113. Altintas, Z.; Gittens, M.; Guerreiro, A.; Thompson, K.A.; Walker, J.; Piletsky, S.; Tothill, I.E. Detection of Waterborne Viruses Using High Affinity Molecularly Imprinted Polymers. *Anal. Chem.* **2015**, *87*, 6801–6807. [[CrossRef](#)]
114. Zhang, F.; Luo, L.; Gong, H.; Chen, C.; Cai, C. A magnetic molecularly imprinted optical chemical sensor for specific recognition of trace quantities of virus. *RSC Adv.* **2018**, *8*, 32262–32268. [[CrossRef](#)]
115. Giamberardino, A.; Labib, M.; Hassan, E.M.; Tetro, J.A.; Springthorpe, S.; Sattar, S.A.; Berezovski, M.V.; DeRosa, M.C. Ultrasensitive norovirus detection using DNA aptasensor technology. *PLoS ONE* **2013**, *8*, 1–9. [[CrossRef](#)] [[PubMed](#)]
116. Escudero-Abarca, B.I.; Suh, S.H.; Moore, M.D.; Dwivedi, H.P.; Jaykus, L.A. Selection, characterization and application of nucleic acid aptamers for the capture and detection of human norovirus strains. *PLoS ONE* **2014**, *9*, e106805.
117. Kim, B.; Chung, K.W.; Lee, J.H. Non-stop aptasensor capable of rapidly monitoring norovirus in a sample. *J. Pharm. Biomed. Anal.* **2018**, *152*, 315–321. [[CrossRef](#)]



© 2020 by the authors. Licensee MDPI, Basel, Switzerland. This article is an open access article distributed under the terms and conditions of the Creative Commons Attribution (CC BY) license (<http://creativecommons.org/licenses/by/4.0/>).